Results on the Asymptotic Stability Properties of Desynchronization in Impulse-coupled Oscillators

Sean Phillips and Ricardo G. Sanfelice

Abstract— The property of desynchronization in impulse-coupled oscillators is studied. Each impulsive oscillator is modeled as a hybrid system with a single timer state that self-resets to zero when it reaches a threshold, at which point any other impulsive oscillator adjusts their timers following a common law. This law dictates the reaction to an external reset. In this setting, desynchronization is considered as timers having equal separation among each other and between successive resets. We show that, for the considered model, desynchronization is an (almost global) asymptotic stability property, which, due to the regularity properties of the hybrid systems, is robust to small perturbations. To establish this result, we recast desynchronization as a set stabilization problem and employ Lyapunov stability tools for hybrid systems. The results are illustrated in examples and simulations.

I. INTRODUCTION

Impulse-coupled oscillators are systems that continuously evolve until a state-triggered event occurs. Networks of such oscillators have been used to model the dynamics of a wide range of biological systems, including fireflies, neurons, cyclic behaviors, and even muscle cells [1], [2], [3]. Such networks have been found to synchronize their variables, by conveying only a small amount of information between the oscillators.

The dual of synchronization is desynchronization. In simple terms, desynchronization in multi-agent systems is the notion that the agents' actions are separated as far apart as possible, similar to clustering or splay-state configurations [4], [5]. For impulse-coupled oscillators, which is the class of systems this paper addresses, desynchronization is the configuration in which all oscillators are evenly spread out while oscillating at the same rate [6]. This action is seen in nature [7] and in neural networks [8], [9]. Desynchronization of oscillators has recently been shown to be of importance in the understanding of Parkinson's disease; see, e.g., [10], [11]. It is also an important property in wireless digital networks [12] and for round-robin scheduling in sensor networks [13].

The approach taken in this paper consists of modeling a network of impulse-coupled oscillators as a hybrid system. The dynamics of the hybrid system capture the (linear) continuous evolution of the timers as well their impulsive/discontinuous behavior due to internal and external events. Analysis of the asymptotic stability properties of the solutions to these systems is performed using the

framework of hybrid systems in [14], [15]. To this end, we recast the study of desynchronization as a set stabilization problem. Unlike synchronization, for which the set of points to stabilize is obvious, the complexity of desynchronization requires first to determine such a collection of points, which we refer to as the *desynchronization set*. We propose an algorithm to compute such a set of points. Then, using Lyapunov stability theory for hybrid systems, we prove that the desynchronization set is asymptotically stable. Details of the analysis for the cases of two and three impulse-coupled oscillators are given. In our context, asymptotic stability of the desynchronization set implies that the distance between the states and the set converge to zero as the amount of time and number of jumps gets large. We define a Lyapunov function as the distance between the state and (an inflated version of) the desynchronization set. We characterize the time for the state to reach a neighborhood of the said set and verify the results numerically.

The remainder of the paper is organized as follows. Section II is devoted to hybrid modeling of impulse-coupled oscillators. Section III-A introduces an algorithm to determine the desynchronization set. Section III-B presents the stability results while the time to convergence is characterized in Section III-C. Section III-D presents numerical results. Final remarks are given in Section IV.

Notation: We use the following notation: $\mathbb{R}$ denotes the real numbers space. $\mathbb{R}^n$ denotes the n-dimensional Euclidean space. $\mathbb{N}$ denotes the natural numbers including zero. Given an interval $\mathcal{S} = [0, t]$ and $n \in \mathbb{N} \setminus \{0\}$, $\mathcal{S}^n$ is the cartesian product of the interval, i.e., $[0, t]^3 = [0, t] \times [0, t] \times [0, t]$. Finally, $\mathbb{B}$ is the closed unit ball centered around the origin in Euclidean space. The Euclidean distance from $x \in \mathbb{R}^n$ and a set $S \subset \mathbb{R}^n$ is denoted by $d(x, S)$. A column vector of N ones is denoted by $\mathbf{1}$. The c-level set of $V : \operatorname{dom} V \to \mathbb{R}$ is given by $L_V(c) = \{x : V(x) = c\}$. The c-sublevel set of V is given by $\tilde{L}_V(c) = \{x : V(x) \leq c\}$.

II. HYBRID MODEL OF IMPULSE-COUPLED OSCILLATORS

A. Overview

In this paper, each impulse-coupled oscillator has a continuous state defining its internal timer. Once any of the oscillator's timer reaches a threshold, it triggers an impulse and reset to zero. At such event, all the other impulse-coupled oscillators decrease their timer by an amount given by $(1+\varepsilon)$ times the value of their timer, where $\varepsilon \in (-1, 0)$.[1] Figure 1

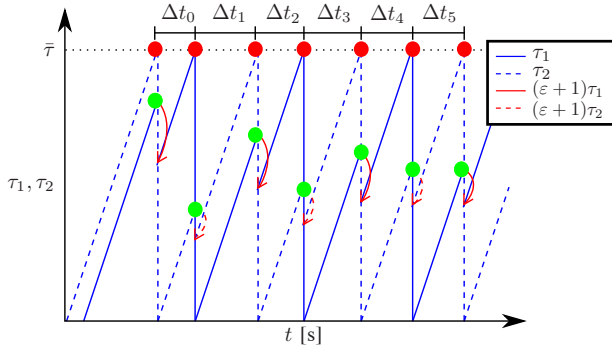[1] Cf. the model for synchronization in [2] where $\varepsilon > 0$.

Fig. 1. An example of two impulse-coupled oscillators reaching desynchronization as Δt_i converges to a constant. The internal resets (red circles) reset the timers to zero. The external resets (green circles) reset the timers to a fraction $(1+\varepsilon)$ of their current value.

shows a trajectory of two impulse-coupled oscillators with states τ_1 and τ_2. In this figure, the red circles indicate when a timer state has reached the threshold (denoted $\bar{\tau}$) and thus resets to zero. The green circles indicate when an oscillator is externally reset and, hence, decreases its timer by $(1+\varepsilon)$ times its current state.

B. Hybrid Modeling

Following the overview in Section II-A, the dynamics of the impulse-coupled oscillators involve impulses and timer resets, which are treated as true discrete events and instantaneous updates, while the smooth evolution of the timer before/after these events define the continuous dynamics. We follow the hybrid formalism of [14], [15], where a hybrid system is given by four objects (C, f, D, G) defining its *data*:

- *Flow map:* a single-valued map $f : \mathbb{R}^n \to \mathbb{R}^n$ defining the flows (or continuous evolution).
- *Flow set:* a set $C \subset \mathbb{R}^n$ specifying the points where flows are possible.
- *Jump map:* a set-valued map $G : \mathbb{R}^n \rightrightarrows \mathbb{R}^n$ defining the jumps (or discrete evolution).
- *Flow set:* a set $D \subset \mathbb{R}^n$ specifying the points where jumps are possible.

A hybrid system capturing the dynamics of the impulse-coupled oscillators is denoted as $\mathcal{H}_N := (C, f, D, G)$ and can be written in the compact form

$$\mathcal{H}_N : \quad \tau \in \mathbb{R}^N \quad \begin{cases} \dot{\tau} = f(\tau) & \tau \in C \\ \tau^+ \in G(\tau) & \tau \in D \end{cases}, \quad (1)$$

where $N \in \mathbb{N} \setminus \{0, 1\}$ is the number of impulse-coupled oscillators. The state of $\mathcal{H}_N$ is given by

$$\tau := [\tau_1 \ \tau_2 \ \dots \ \tau_N]^\top \in P^N := [0, \bar{\tau}]^N.$$

The flow and jump sets are defined to constrain the evolution of the timers. The flow set is defined by

$$C := \{\tau \in P^N \ : \ \tau_i \in [0, \bar{\tau}], \forall \ i \in I\} \ (= [0, \bar{\tau}]^N = P^N), \quad (2)$$

where $I := \{1, 2, \dots, N\}$ and $\bar{\tau} > 0$ is the threshold. During flows, the timers simply count ordinary time. Then, the flow map is defined as

$$f(\tau) := \mathbf{1} \qquad \forall \tau \in C.$$

The impulsive events described in Section II-A are modeled by a jump map G. Jumps occur when the state is in the jump set D, e.g., belongs to the set

$$D := \{\tau \in P^N \ : \ \exists i \in I \text{ s.t. } \tau_i = \bar{\tau}\}. \quad (3)$$

From such points, the i-th timer will be reset to zero and force a jump of all other timers. Such discrete dynamics are captured by the following jump map: for each $\tau \in D$ define $G(\tau) = [g_1(\tau) \ g_2(\tau) \ \dots \ g_N(\tau)]^\top$, where

$$g_i(\tau) = \begin{cases} 0 & \text{if } \tau_i = \bar{\tau}, \tau_j < \bar{\tau} \ \forall j \in I \setminus \{i\} \\ \{0, \tau_i(1+\varepsilon)\} & \text{if } \tau_i = \bar{\tau} \ \exists j \in I \setminus \{i\} \text{ s.t. } \tau_j = \bar{\tau} \\ (1+\varepsilon)\tau_i & \text{if } \tau_i < \bar{\tau} \ \exists j \in I \text{ s.t. } \tau_j = \bar{\tau} \end{cases} \quad (4)$$

with parameters $\varepsilon \in (-1, 0)$ and $\bar{\tau} > 0$. When a jump is triggered by the jump set, the state τ_i jumps according to the i-th component of the jump map g_i. When a state reaches the threshold $\bar{\tau}$, it is reset to zero only when all other states are less than that threshold; otherwise, if multiple timers reach the threshold simultaneously, the jump map is set valued to indicate that either $g_i(\tau) = 0$ or $g_i(\tau) = (1+\varepsilon)\tau_i$ is possible. This is to ensure that the jump map satisfies the regularity conditions outlined in Section II-C[2].

Solutions to the hybrid system $\mathcal{H}_N$ evolve continuously (flow) and/or discretely (jump) depending on the continuous and discrete dynamics and the sets where those dynamics apply. As in [15], we treat the number of jumps as an independent variable j and the amount of time of flows by the independent variable t. Then, solutions τ to $\mathcal{H}_N$ are given by *hybrid arcs* parameterized by (t, j) which takes values on the *hybrid time domain* $\operatorname{dom} \tau$; see [14], [15] for more details.[3]

C. Basic Properties of $\mathcal{H}_N$

To apply analysis tools for hybrid systems, which will be presented in Section III, the data of the hybrid system $\mathcal{H}_N$ must meet certain mild conditions. These conditions, referred to as *hybrid basic conditions*, are as follows:

- A1) C and D are closed sets in $\mathbb{R}^N$.
- A2) $f : \mathbb{R}^N \to \mathbb{R}^N$ is continuous on C.
- A3) $G : \mathbb{R}^N \rightrightarrows \mathbb{R}^N$ is an outer semicontinuous[4] set-valued mapping, locally bounded on D, and such that $G(x)$ is nonempty for each $x \in D$.

Lemma 2.1: $\mathcal{H}_N$ satisfies the hybrid basic conditions.

Note that satisfying the hybrid basic conditions allow for this hybrid system to be considered as well-posed which automatically gives robustness to vanishing state disturbances, see [14], [15].

---

[2]In [4], a more general flow map and a jump map incrementing τ_i by $\varepsilon > 0$ are considered.

[3]A solution τ is said to be *nontrivial* if $\operatorname{dom} \tau$ contains at least one point different from $(0, 0)$, *maximal* if there does not exist a solution τ' such that τ is a truncation of τ' to some proper subset of $\operatorname{dom} \tau'$, *complete* if $\operatorname{dom} \tau$ is unbounded, and *Zeno* if it is complete but the projection of $\operatorname{dom} \tau$ onto $\mathbb{R}_{\geq 0}$ is bounded.

[4]A set-valued mapping $G : \mathbb{R}^N \rightrightarrows \mathbb{R}^N$ is *outer semicontinuous* if its graph $\{(x, y) : x \in \mathbb{R}^n, y \in G(x)\}$ is closed.

## III. ASYMPTOTIC STABILITY PROPERTIES OF $\mathcal{H}_N$

Our goal is to show that the desynchronization configuration is asymptotically stable. A precise definition of asymptotic stability for hybrid systems $\mathcal{H}_N$ is given in [14], [15] and is defined as the property of a set being both stable and attractive. The set of points from where the attractivity property holds is the basin of attraction and excludes all points where the system trajectories never converge to desynchronization. The basin of attraction for $\mathcal{H}_N$ does not include any point τ such that any two or more timers are equal or after a jump become equal. This set is denoted by $\mathcal{X}_N$ and is defined as

$$\mathcal{X}_N := \bigcup_{i,j \in I, i \neq j} \left(\{\tau \in P^N : \tau_i = \tau_j\} \right.$$
$$\left. \cup \{\tau \in D : \tau_i = g_j(\tau)\} \right).$$

For example, consider the case $N = 2$, i.e., $\mathcal{H}_2$. Then the set $\mathcal{X}_2$ is defined as

$$\mathcal{X}_2 = \{\tau \in P^2 : \tau_1 = \tau_2\} \cup \{\tau \in D : g_1(\tau) = \tau_2\}$$
$$\cup \{\tau \in D : g_2(\tau) = \tau_1\}. \quad (5)$$

This set defines the line $\tau_1 = \tau_2$ and the points $\{(0, \bar{\tau}), (\bar{\tau}, 0)\}$, see Figure 2(a).
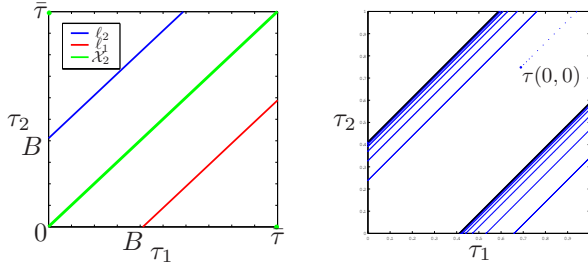
(a) The sets $\mathcal{X}_2$ and $\mathcal{A}_2$. The set $\mathcal{A}_2$ defined by the union of ℓ_1 and ℓ_2.

(b) Simulation trajectory (blue) of τ_1, τ_2 for the hybrid system $\mathcal{H}_2$ showing convergence to the set $\mathcal{A}_2$ (black)

Fig. 2. Sets associated with $\mathcal{H}_2$ and a solution to it from $\tau(0,0) = [0.7, 0.75]^\top$ with $\varepsilon = 0.3$ and $\bar{\tau} = 1$.

A. Construction of set $\mathcal{A}_N$ for $\mathcal{H}_N$

In this section, we identify the set of points corresponding to the impulse-coupled oscillators being desynchronized, namely, the desynchronization set. We define desynchronization as the behavior in which the separation between all of the timers' impulses is maximized. It leads to an ordered sequence of impulse times with equal separation. The desynchronization set for the hybrid system $\mathcal{H}_N$ is denoted as $\mathcal{A}_N$ and will be parameterized by ε, threshold $\bar{\tau}$, and the number of impulse-coupled oscillators N.

To compute this set, first we provide some basic intuition about the dynamics of $\mathcal{H}_N$ when desynchronized. The set $\mathcal{A}_N$ must be forward invariant. Hence, the definition of the constant flow map f admits a set in the form of "lines" ℓ_k, each of them with the direction $\mathbf{1}$ intersecting the jump set at a point which, for the k-th line, we denote as $\widetilde{\tau}^k$. Then, the

desynchronization set is given by the union of sets ℓ_k defined by points $\tau = \widetilde{\tau}^k + \mathbf{1}s \in P^N$ parameterized by $s \in \mathbb{R}$. To identify $\widetilde{\tau}^k$, consider a point $\widetilde{\tau}^k \in D \setminus \mathcal{X}_N$ with components satisfying $\widetilde{\tau}_1^k = \bar{\tau} > \widetilde{\tau}_2^k > \widetilde{\tau}_3^k > ... > \widetilde{\tau}_N^k$. This point belongs to $\mathcal{A}_N$ only if the distance between the expiring timer ($\widetilde{\tau}_1^k$) and each of its other components ($\widetilde{\tau}_i^k$, $i \in I \setminus \{1\}$) is equal to the distance between the value after the jump of the timer expiring next ($\widetilde{\tau}_2^{k+}$) and the value after the jump of its other components ($\widetilde{\tau}_i^{k+}$, $i \in I \setminus \{2\}$), respectively. More precisely,

$$\widetilde{\tau}_1^k - \widetilde{\tau}_i^k = \widetilde{\tau}_2^{k+} - \widetilde{\tau}_{\text{next}(i)}^{k+} \qquad \forall\, i \in I \setminus \{1\}, \quad (6)$$

where $\widetilde{\tau}^{k+} = G(\widetilde{\tau}^k)$ and $\text{next}(i) = i + 1$ if $i + 1 \leq N$ and 1 otherwise. Since $\mathcal{X}_N$ contains all points such that at least two or more timers are the same, we can consider the case when one component of $\widetilde{\tau}^k$ is equal to $\bar{\tau}$ at a time. For each such case, we have $(N - 1)!$ possible permutations of the other components and N possible timer components equal to $\bar{\tau}$, leading to $N!$ total possible sets ℓ_k. To illustrate the algorithm outlined above for the construction of $\mathcal{A}_N$, consider the case of $N = 2$ and $\widetilde{\tau}_1^1 = \bar{\tau} > \widetilde{\tau}_2^1$. For $i = 2$, (6) becomes

$$\bar{\tau} - \widetilde{\tau}_2^1 = \widetilde{\tau}_2^1(\varepsilon + 1)$$

which leads to $\widetilde{\tau}_2^1 = \frac{\bar{\tau}}{\varepsilon+2}$ and it follows that $\widetilde{\tau}^1 = [\bar{\tau}, \frac{\bar{\tau}}{\varepsilon+2}]^\top$. Similarly for $\widetilde{\tau}_2^1 = \bar{\tau} > \widetilde{\tau}_1^1$, we get from (6) the equation $\bar{\tau} - \widetilde{\tau}_1^1 = \widetilde{\tau}_2^1(\varepsilon + 1)$ which implies $\widetilde{\tau}^2 = [\frac{\bar{\tau}}{\varepsilon+2}, \bar{\tau}]^\top$. A glimpse at the case for $N = 3$ with $\widetilde{\tau}_1^1 = \bar{\tau} > \widetilde{\tau}_2^1 > \widetilde{\tau}_3^1$, (6) leads to

$$\bar{\tau} - \widetilde{\tau}_2^1 = \widetilde{\tau}_2^1(1 + \varepsilon) - \widetilde{\tau}_3^1(1 + \varepsilon),$$
$$\bar{\tau} - \widetilde{\tau}_3^1 = \widetilde{\tau}_2^1(1 + \varepsilon) - 0.$$

The solution to these equations is $\widetilde{\tau}^1 = [\bar{\tau}, \bar{\tau}(\varepsilon + 2)/(\varepsilon^2 + 3\varepsilon + 3), \bar{\tau}/(\varepsilon^2 + 3\varepsilon + 3)]^\top$.

The algorithm above for the N case results in the system of equations $\Gamma \tau_s = b$, where τ_s is the state $\widetilde{\tau}^k$ sorted into decreasing order. For example, if $\widetilde{\tau}^k$ is such that $\widetilde{\tau}_2^k = \bar{\tau} > \widetilde{\tau}_1^k > \widetilde{\tau}_3^k$, then τ_s is given as $[\widetilde{\tau}_2^k, \widetilde{\tau}_1^k, \widetilde{\tau}_3^k]^\top$. The matrices Γ and b are given by

$$\Gamma = \begin{bmatrix} 1 & 0 & 0 & 0 & 0 \\ 0 & (2+\varepsilon) & -(1+\varepsilon) & \dots & 0 \\ 0 & (1+\varepsilon) & 1 & \ddots & \vdots \\ \vdots & \vdots & \vdots & \ddots & -(1+\varepsilon) \\ 0 & (1+\varepsilon) & 0 & \dots & 1 \end{bmatrix} \quad (7)$$

and

$$b = \bar{\tau}\mathbf{1}. \quad (8)$$

It can be shown that Γ is invertible for any $\varepsilon \in (-1, 0)$. Then, the solution τ_s needs to be unsorted and becomes $\widetilde{\tau}^k$ in the definition of the set ℓ_k.

The solution to $\Gamma \tau_s = b$ is the result of a single case of $\tau \in D \setminus \mathcal{X}_N$. As indicated above, to get a full definition of the set $\mathcal{A}_N$, the $N!$ sets ℓ_k should be computed. For arbitrary N, the set $\mathcal{A}_N$ is given as a collection of sets ℓ_k given by

$$\mathcal{A}_N = \bigcup_{k=1}^{N!} \ell_k, \quad (9)$$

where, for each $k \in \{1, 2, \ldots, N!\}, \ell_k := \{\tau : \tau = \widetilde{\tau}^i + \mathbf{1}s \in P^N, s \in \mathbb{R}\}$. For the case $N = 2$, the points $\widetilde{\tau}_k$ for $k \in \{1, 2\}$ lead to the set $\mathcal{A}_2$ given by

$$\mathcal{A}_2 = \ell_1 \cup \ell_2 = \left\{\tau : \tau = \begin{bmatrix} \bar{\tau} \\ \frac{\bar{\tau}}{\varepsilon+2} \end{bmatrix} + \mathbf{1}s \in P^N, s \in \mathbb{R}\right\}$$
$$\cup \left\{\tau : \tau = \begin{bmatrix} \frac{\bar{\tau}}{\varepsilon+2} \\ \bar{\tau} \end{bmatrix} + \mathbf{1}s \in P^N, s \in \mathbb{R}\right\}.$$

Figure 2(a) shows these sets in the (τ_1, τ_2)-plane. Figure 2(b) shows a solution to $\mathcal{H}_2$. The initial conditions for the simulation are $\tau(0, 0) = (0.75, \ 0.7)$.

B. Lyapunov Stability

Lyapunov theory for hybrid systems is employed to show that the set of points $\mathcal{A}_N$ is asymptotically stable.

1) Lyapunov Stability Analysis for $\mathcal{H}_2$: Section III-A arrived to the set given by $\mathcal{A}_2 = \ell_1 \cup \ell_2$ for the hybrid system $\mathcal{H}_2$. Our goal is to use a Lyapunov function to establish, via [15, Theorem 23], that the desynchronization set is (almost) globally asymptotically stable for $\mathcal{H}_2$. Consider the Lyapunov function V_2 given by the distance from τ to $\mathcal{A}_2$. The desynchronization set must be inflated to avoid situations where there may be an increase in distance during flows near the corners $\{(0, 0), (\bar{\tau}, \bar{\tau})\}$, see Figure 2(a). From the figure, as solutions flow to points near $\{\bar{\tau}, \bar{\tau}\}$, the minimum distance to the lines ℓ_k will increase due to the fact that the lines live in P^2. Then, we define

$$\widetilde{\mathcal{A}}_2 := \widetilde{\ell}_1 \cup \widetilde{\ell}_2 \supset \mathcal{A}_2,$$

where $\widetilde{\ell}_1$ and $\widetilde{\ell}_2$ are extensions of ℓ_1 and ℓ_2 given by

$$\widetilde{\ell}_1 = \{\tau : \tau = \begin{bmatrix} \bar{\tau} \\ \frac{\bar{\tau}}{\varepsilon+2} \end{bmatrix} + \mathbf{1}s \in P^2 \cup \sqrt{2}\bar{\tau}\mathbb{B}, s \in \mathbb{R}\},$$
$$\widetilde{\ell}_2 = \{\tau : \tau = \begin{bmatrix} \frac{\bar{\tau}}{\varepsilon+2} \\ \bar{\tau} \end{bmatrix} + \mathbf{1}s \in P^2 \cup \sqrt{2}\bar{\tau}\mathbb{B}, s \in \mathbb{R}\}. \tag{10}$$

The proposed Lyapunov function is given by

$$V_2(\tau) = |\tau|_{\widetilde{\mathcal{A}}_2} = \min\left\{d(\tau, \widetilde{\ell}_1), d(\tau, \widetilde{\ell}_2)\right\} \ \forall \tau \in P_2 \backslash (\widetilde{\mathcal{A}}_2 \cup \mathcal{X}_2) \tag{11}$$

with $\mathcal{X}_2$ defined as in (5). The Lyapunov function (11) is the minimum distance from the state to the union of the sets $\widetilde{\ell}_1$ and $\widetilde{\ell}_2$. The distance between a point τ and $\widetilde{\ell}_k$, in $\mathbb{R}^2$, is given by $d(\tau, \widetilde{\ell}_k) = \left|(\widetilde{\tau}^k - \tau) - \frac{(\widetilde{\tau}^k - \tau)^\top \mathbf{1}}{2}\right|$, where $\widetilde{\tau}^k$ corresponds to $\widetilde{\ell}_k$. Then, $d(\tau, \widetilde{\ell}_k)$ reduces to

$$d(\tau, \widetilde{\ell}_k) = \frac{1}{\sqrt{2}}|\tau_1 - \tau_2 + (\widetilde{\tau}_2^k - \widetilde{\tau}_1^k)|. \tag{12}$$

Using the expressions in (10), then V_2 in (11) reduces to

$$V_2(\tau) = |\tau|_{\widetilde{\mathcal{A}}_2} = \frac{1}{\sqrt{2}}\min\{|\tau_2 - \tau_1 - B|, |\tau_2 - \tau_1 + B|\} \ \forall \tau \in P^2 \tag{13}$$

where $B = \frac{\varepsilon+1}{\varepsilon+2}\bar{\tau}$.

Along flows, we have that for each $\tau \in C \setminus (\widetilde{\mathcal{A}}_2 \cup \mathcal{X}_2)$ and each $k \in \{-B, B\}$,

$$\begin{aligned} \langle \nabla V_2(\tau), f(\tau) \rangle &= \left\langle \frac{1}{\sqrt{2}}\nabla |\tau_2 - \tau_1 + k|, [1, \ 1]^\top \right\rangle \\ &= \frac{1}{\sqrt{2}}\langle [\mp 1, \ \pm 1]^\top, [1, \ 1]^\top \rangle \\ &= \mp\frac{1}{\sqrt{2}} \pm \frac{1}{\sqrt{2}} \\ &= 0. \end{aligned}$$

Then, it follows that

$$\langle \nabla V_2(\tau), f(\tau) \rangle = 0 \quad \forall \tau \in C \setminus (\widetilde{\mathcal{A}}_2 \cup \mathcal{X}_2).$$

We now evaluate V_2 at jumps, that is, $\Delta V_2(\tau) = V_2(G(\tau)) - V_2(\tau)$. Considering the case when $\tau \in D \setminus (\widetilde{\mathcal{A}}_2 \cup \mathcal{X}_2)$, with $\tau_1 = \bar{\tau} > \tau_2$ leads to $g_1(\tau) = 0$ and $g_2(\tau) = (1+\varepsilon)\tau_2$. Note that $V_2(\tau) = d(\tau, \widetilde{\ell}_1) = \frac{1}{\sqrt{2}}\left|\tau_2 - \frac{\bar{\tau}}{\varepsilon+2}\right|$ and $|(1+\varepsilon)\tau_2 - B| < |(1+\varepsilon)\tau_2 + B|$. Then, we have

$$\begin{aligned} \sqrt{2}\Delta V_2(\tau) &= \min\{|g_2(\tau) + B|, |g_2(\tau) - B|\} \\ &\quad - \min\{|\tau_2 - \bar{\tau} + B|, |\tau_2 - \bar{\tau} - B|\} \\ &= |(1+\varepsilon)\tau_2 - B| - |\tau_2 - \bar{\tau} + B| \\ &= \left|(1+\varepsilon)\tau_2 - \frac{\varepsilon+1}{\varepsilon+2}\bar{\tau}\right| - \left|\tau_2 - \bar{\tau} + \frac{\varepsilon+1}{\varepsilon+2}\bar{\tau}\right| \\ &= \varepsilon\left|\tau_2 - \frac{\bar{\tau}}{\varepsilon+2}\right| \end{aligned}$$

Similarly, consider the case when $\tau \in D \setminus (\widetilde{\mathcal{A}}_2 \cup \mathcal{X}_2)$, with $\tau_2 = \bar{\tau} > \tau_1$. After the jump, we have $g_2(\tau) = 0$ and $g_1(\tau) = (1+\varepsilon)\tau_1$. Then, similarly,

$$\begin{aligned} \sqrt{2}\Delta V_2(\tau) &= \min\{| -g_1(\tau) + B|, | -g_1(\tau) - B|\} \\ &\quad - \min\{|\bar{\tau} - \tau_1 + B|, |\bar{\tau} - \tau_1 - B|\} \\ &= |-(1+\varepsilon)\bar{\tau} + B| - |\bar{\tau} - \tau_1 - B| \\ &= \left|-(1+\varepsilon)\bar{\tau} + \frac{\varepsilon+1}{\varepsilon+2}\bar{\tau}\right| - \left|\bar{\tau} - \tau_1 - \frac{\varepsilon+1}{\varepsilon+2}\bar{\tau}\right| \\ &= \varepsilon\left|\tau_1 + \frac{\bar{\tau}}{\varepsilon+2}\right| \end{aligned}$$

Combining the above calculations, we have

$$V_2(G(\tau)) - V_2(\tau) = \varepsilon V_2(\tau) < 0 \quad \forall \tau \in D \setminus (\widetilde{\mathcal{A}}_2 \cup \mathcal{X}_2).$$

Since we have this property at jumps, there is no complete solution to $\mathcal{H}_2$ that remains in $L_{V_2}(\mu)$ for $\mu > 0$. From [15, Theorem 23], we have that $\widetilde{\mathcal{A}}_2$ is asymptotically stable for $\mathcal{H}_2$. Since the set $(C \cup D) \backslash (\mathcal{X}_2 \cup \widetilde{\mathcal{A}}_2)$ is compact and forward invariant, we have that the basin of attraction for $\widetilde{\mathcal{A}}_2$ contains every point in $(C \cup D) \setminus \mathcal{X}_2$, and the points $\tau \in C \cup D$ that do not converge to $\widetilde{\mathcal{A}}_2$ are in $\mathcal{X}_2$. Finally, since $\mathcal{A}_2 \subset \widetilde{\mathcal{A}}_2$ and there are no solutions from $\widetilde{\mathcal{A}}_2 \setminus \mathcal{A}_2$, we have that the stability properties of $\widetilde{\mathcal{A}}_2$ are transferred to $\mathcal{A}_2$ (though V_2 in (11) is not a Lyapunov function certifying such property for $\mathcal{A}_2$).

Remark 3.1: The analysis above excluded all points where the jump map is set valued, i.e., when $\tau \in \mathcal{X}_2$. We can

further show that not all solutions remain in $\mathcal{X}_2$ for all (t, j). For example, if $\tau(0, 0) = [\bar{\tau}, \bar{\tau}]^\top \in D \cap \mathcal{X}_2$, then there are nonunique solutions. After the jump,

$$G(\tau) = (\{0, \tau_1(1 + \varepsilon)\}, \{0, \tau_2(1 + \varepsilon)\}),$$

which leads to any of the following four options of the state after such a jump: $(0, 0), (0, \bar{\tau}(1 + \varepsilon)), (\bar{\tau}(1 + \varepsilon), 0)$, and $(\bar{\tau}(1 + \varepsilon), \bar{\tau}(1 + \varepsilon))$. If the state chooses either $(0, 0)$ or $(\bar{\tau}(1+\varepsilon), \bar{\tau}(1+\varepsilon))$, then the state is mapped back to $\mathcal{X}_2$. But, if either one of the other options are chosen, then $G(\tau) \notin \mathcal{X}_2$ because $\tau_1 \neq \tau_2$ and the solution will converge to the set $\mathcal{A}_2$. In fact, the only solutions that never desynchronize are those that continuously pick $(0, 0)$ or $(\bar{\tau}(1+\varepsilon), \bar{\tau}(1+\varepsilon))$ at jumps.

2) Lyapunov Stability Analysis for $\mathcal{H}_3$: For the case when $N = 3$, we have a state vector given by $\tau = [\tau_1, \tau_2, \tau_3]^\top$ and a Lyapunov function can be defined as $V_3(\tau) = |\tau|_{\widetilde{\mathcal{A}}_3} = \min\{d(\tau, \widetilde{\ell}_1), \ldots, d(\tau, \widetilde{\ell}_6)\}$, where $d(\tau, \widetilde{\ell}_k) = |(\widetilde{\tau}^k - \tau) - ((\widetilde{\tau}^k - \tau)^\top \mathbf{1})\mathbf{1}/3|$ and each inflation of the set ℓ^k is defined as $\widetilde{\ell}_k := \{\tau : \tau + \widetilde{\tau}^k + \mathbf{1}s \in P^3 \cup \sqrt{3}\bar{\tau}\mathbb{B}, s \in \mathbb{R}\}$. Then we can use [15, Theorem 23] to establish (almost) global asymptotic stability for $\widetilde{\mathcal{A}}_3$. It follows that for each $\tau \in C \setminus (\mathcal{X}_3 \cup \widetilde{\mathcal{A}}_3)$, $\langle \nabla V_3(\tau), f(\tau) \rangle = 0$. During jumps, consider the case of $\tau_1 = \bar{\tau} > \tau_2 > \tau_3$ and $V_3(\tau) = d(\tau, \widetilde{\ell}_1)$. Then, after the jump, $G(\tau) = [0, (1 + \varepsilon)\tau_2, (1 + \varepsilon)\tau_3]^\top$ with $\tau_2 > \tau_3$ and $V_3(G(\tau)) = d(\tau, \widetilde{\ell}_4)$. From (6), the $\widetilde{\tau}^k$ corresponding to each $\widetilde{\ell}_k$ is $\widetilde{\tau}^1 = [\bar{\tau}, (\varepsilon + 2)\bar{\tau}/(\varepsilon^2 + 3\varepsilon + 3), \bar{\tau}/(\varepsilon^2 + 3\varepsilon + 3)]^\top$ and $\widetilde{\tau}^4 = [\bar{\tau}/(\varepsilon^2 + 3\varepsilon + 3), \bar{\tau}, (\varepsilon + 2)\bar{\tau}/(\varepsilon^2 + 3\varepsilon + 3)]^\top$. It follows that

$$V_3(\tau) = \left| (\widetilde{\tau}^1 - \tau) - \frac{(\widetilde{\tau}^1 - \tau)^\top \mathbf{1}}{3}\mathbf{1} \right|$$

$$= \left\| \begin{bmatrix} \bar{\tau} - \bar{\tau} - \frac{1}{3}\left(\frac{\varepsilon+3}{(\varepsilon^2+3\varepsilon+3)}\bar{\tau} - \tau_2 - \tau_3 \right) \\ \frac{(\varepsilon+2)\bar{\tau}}{(\varepsilon^2+3\varepsilon+3)} - \tau_2 - \frac{1}{3}\left(\frac{\varepsilon+3}{(\varepsilon^2+3\varepsilon+3)}\bar{\tau} - \tau_2 - \tau_3 \right) \\ \frac{\bar{\tau}}{(\varepsilon^2+3\varepsilon+3)} - \tau_3 - \frac{1}{3}\left(\frac{\varepsilon+3}{(\varepsilon^2+3\varepsilon+3)}\bar{\tau} - \tau_2 - \tau_3 \right) \end{bmatrix} \right\|$$

$$= \left\| \begin{bmatrix} \frac{-(\varepsilon+3)\bar{\tau}}{3(\varepsilon^2+3\varepsilon+3)} + \frac{\tau_2}{3} + \frac{\tau_3}{3} \\ \frac{(2\varepsilon+3)\bar{\tau}}{3(\varepsilon^2+3\varepsilon+3)} + \frac{2\tau_2}{3} + \frac{\tau_3}{3} \\ \frac{-\varepsilon\bar{\tau}}{3(\varepsilon^2+3\varepsilon+3)} + \frac{\tau_2}{3} + \frac{2\tau_3}{3} \end{bmatrix} \right\|.$$

Then, $V_3(G(\tau))$ is given by

$$V_3(G(\tau)) = \left| (\widetilde{\tau}^4 - \tau^+) - \frac{(\widetilde{\tau}^4 - \tau^+)^\top \mathbf{1}}{3}\mathbf{1} \right|$$

$$= \left\| \begin{bmatrix} \frac{3\bar{\tau}}{3(\varepsilon^2+3\varepsilon+3)} - \frac{(\varepsilon^2+4\varepsilon+6)\bar{\tau}}{3(\varepsilon^2+3\varepsilon+3)} + \frac{\tau_2(1+\varepsilon)}{3} + \frac{\tau_3(1+\varepsilon)}{3} \\ \frac{3(\varepsilon^2+3\varepsilon+3)\bar{\tau}}{3(\varepsilon^2+3\varepsilon+3)} - \frac{(\varepsilon^2+4\varepsilon+6)\bar{\tau}}{3(\varepsilon^2+3\varepsilon+3)} + \frac{2(1+\varepsilon)\tau_2}{3} + \frac{\tau_3(1+\varepsilon)}{3} \\ \frac{3(\varepsilon+2)\bar{\tau}}{3(\varepsilon^2+3\varepsilon+3)} - \frac{(\varepsilon^2+4\varepsilon+6)\bar{\tau}}{3(\varepsilon^2+3\varepsilon+3)} + \frac{\tau_2(1+\varepsilon)}{3} + \frac{2(1+\varepsilon)\tau_3}{3} \end{bmatrix} \right\|$$

$$= \left\| \begin{bmatrix} \frac{-(\varepsilon^2+4\varepsilon+3)\bar{\tau}}{3(\varepsilon^2+3\varepsilon+3)} + \frac{\tau_2(1+\varepsilon)}{3} + \frac{\tau_3(1+\varepsilon)}{3} \\ \frac{(2\varepsilon^2+5\varepsilon+3)\bar{\tau}}{3(\varepsilon^2+3\varepsilon+3)} + \frac{2(1+\varepsilon)\tau_2}{3} + \frac{\tau_3(1+\varepsilon)}{3} \\ \frac{-(\varepsilon^2+\varepsilon)\bar{\tau}}{3(\varepsilon^2+3\varepsilon+3)} + \frac{\tau_2(1+\varepsilon)}{3} + \frac{2(1+\varepsilon)\tau_3}{3} \end{bmatrix} \right\|$$

$$= (1 + \varepsilon) \left\| \begin{bmatrix} \frac{-(\varepsilon+3)\bar{\tau}}{3(\varepsilon^2+3\varepsilon+3)} + \frac{\tau_2}{3} + \frac{\tau_3}{3} \\ \frac{(2\varepsilon+3)\bar{\tau}}{3(\varepsilon^2+3\varepsilon+3)} + \frac{2\tau_2}{3} + \frac{\tau_3}{3} \\ \frac{-\varepsilon\bar{\tau}}{3(\varepsilon^2+3\varepsilon+3)} + \frac{\tau_2}{3} + \frac{2\tau_3}{3} \end{bmatrix} \right\|$$

$$= (1 + \varepsilon)V_3(\tau)$$

and for the case of $\tau \in D \setminus (\widetilde{\mathcal{A}}_3 \cup \mathcal{X}_3)$ such that $\tau_1 = \bar{\tau} > \tau_2 > \tau_3$, it follows that $V_3(G(\tau)) - V_3(\tau) = \varepsilon V_3(\tau)$. Similar results can be found for each case of $\tau \in D \setminus (\widetilde{\mathcal{A}}_3 \cup \mathcal{X}_3)$.

Since we have that no complete solutions remain in $L_{V_3}(\mu)$ for $\mu > 0$ and the set $P^3 \setminus (\mathcal{X}_3 \cup \widetilde{\mathcal{A}}_3)$ is compact and forward invariant, the basin of attraction for $\widetilde{\mathcal{A}}_3$ is given by $P^3 \setminus \mathcal{X}_3$. Also, since $\mathcal{A}_3 \subset \widetilde{\mathcal{A}}_3$ and there are no solutions from $\widetilde{\mathcal{A}}_3 \setminus \mathcal{A}_3$ we can conclude that the set $\mathcal{A}_3$ is asymptotically stable with the basin of attraction $P^3 \setminus \mathcal{X}_3$. Similar to Remark 3.1, if the solutions to $\mathcal{H}_3$ are initially in $\mathcal{X}_3$ then they will be nonunique. These solutions have the opportunity to jump out of $\mathcal{X}_3$ at every jump. If this occurs, these such solutions will converge to $\mathcal{A}_3$.

The arguments above lead to the following definition of a Lyapunov function for the N case:

$$V_N(\tau) = |\tau|_{\widetilde{\mathcal{A}}_N} = \min\{d(\tau, \widetilde{\ell}_1), d(\tau, \widetilde{\ell}_2), \ldots, d(\tau, \widetilde{\ell}_{N!})\},$$

where $d(\tau, \widetilde{\ell}_k) = |(\widetilde{\tau}^k - \tau) - ((\widetilde{\tau}^k - \tau)^\top \mathbf{1})\mathbf{1}/N|$, $k \in \{1, 2, \ldots, N!\}$ (note that this function satisfies the regularity properties required by [15, Theorem 23]). The next result follows using arguments similar to those outlined above[5].

Theorem 3.2: For every integer $N > 1$, $\bar{\tau} > 0$, and $\varepsilon \in (-1, 0)$, the hybrid system $\mathcal{H}_N$ is such that $\mathcal{A}_N$ is asymptotically stable with basin of attraction given by $P^N \setminus \mathcal{X}_N$.

C. Characterization of Time of Convergence

In this section, we characterize the time to converge to a neighborhood of $\mathcal{A}_N$. The proposed (upper bound) of the time to converge depends on the initial distance to the set $\mathcal{A}_N$ and the parameters of the hybrid system $(\varepsilon, \bar{\tau})$.

Theorem 3.3: For every integer $N > 1$ and every c_1, c_2 such that $\min_{x \in \mathcal{X}_N} d(x, \mathcal{A}_N) > c_2 > c_1 > 0$, every maximal solution to $\mathcal{H}_N$ with initial conditions $\tau(0, 0) \in \widetilde{L}_{V_N}(c_2)$ is such that

$$\tau(t, j) \in \widetilde{L}_{V_N}(c_1) \quad \forall (t, j) \in \text{dom } \tau, t + j \geq M,$$

where

$$M = (\bar{\tau} + 1)\frac{\log \frac{c_2}{c_1}}{\log \frac{1}{1+\varepsilon}}$$

and $\widetilde{L}_{V_N}(\mu) := \{\tau \in C \cup D : V_N(\tau) \leq \mu\}$.

Figure 3 shows the time to converge (divided by $\bar{\tau} + 1$) versus ε with constant $c_2 = 0.99\bar{\tau}$ and varying values of c_1. As the figure indicates, the time to converge decreases as $|\varepsilon|$ increases, which confirms the intuition that the larger the jump the faster oscillators desynchronize. Some performance analysis was for impulse-coupled oscillators with communication constraints in [16].

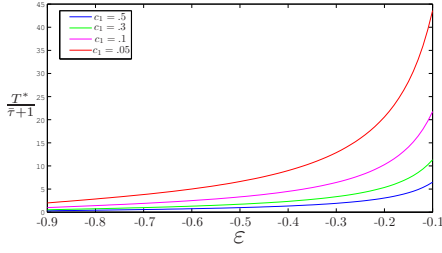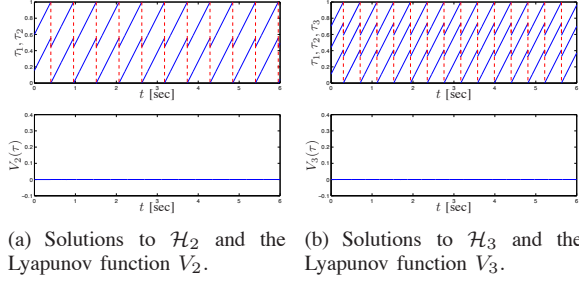[5]Cf. the global attractivity property of the model in [4].

Fig. 3. Time to converge (over $\bar{\tau} + 1$) as a function of $\varepsilon \in [-0.9, -0.1]$, with $c_2 = 0.99\bar{\tau}$ and $c_1 \in \{0.5\bar{\tau}, 0.3\bar{\tau}, 0.1\bar{\tau}, 0.05\bar{\tau}\}$

(a) Solutions to $\mathcal{H}_2$ and the Lyapunov function V_2.

(b) Solutions to $\mathcal{H}_3$ and the Lyapunov function V_3.

Fig. 4. Solutions to $\mathcal{H}_N$ for $N \in \{2, 3\}$ that are initially in the set $\mathcal{A}_N$ and Lyapunov function evaluated along solutions.

D. Numerical Analysis

The possible solutions to the hybrid system $\mathcal{H}_N$ fall into three categories: always desynchronized, asymptotically desynchronized, and never desynchronized. The following simulation results show the evolution of solutions for each category. The parameters used in these simulations are $\bar{\tau} = 1$ and $\varepsilon = -0.2$.

1) **Always desynchronized** ($N \in \{2, 3\}$)**:** A solution to $\mathcal{H}_N$ that has initial condition $\tau(0, 0) \in \mathcal{A}_N$ stays desynchronized. Figure 4 shows the evolution of such a solution for systems $\mathcal{H}_2$ and $\mathcal{H}_3$. Furthermore, as also shown in the figures, for these solutions the Lyapunov function is initially zero and stays zero as time goes on.

2) **Asymptotically desynchronized** ($N \in \{2, 3, 7, 10\}$)**:** A solution of $\mathcal{H}_N$ that starts in $P^N \setminus (\mathcal{X}_N \cup \mathcal{A}_N)$ asymptotically converges to $\mathcal{A}_N$ as Theorem 3.3 indicates. Figure 5 shows both $\mathcal{H}_2$ and $\mathcal{H}_3$ converging to $\mathcal{A}_2$ and $\mathcal{A}_3$, respectively.

For $\mathcal{H}_2$, if $\tau(0, 0) = [0, 0.1]^\top$, then the initial sublevel set is $\widetilde{L}_{V_2}(0.34)$. Using Theorem 3.3, the time to converge to the sublevel set $\widetilde{L}_{V_2}(0.1)$ leads to $M = 7.98$. Figure 5(a) shows
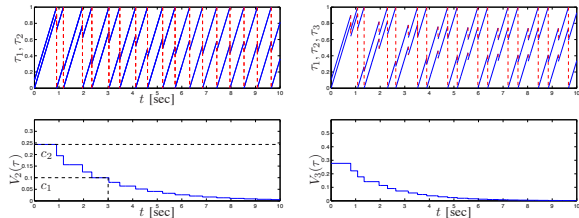
(a) Solutions to $\mathcal{H}_2$ such that $c_2 = 0.34$ with $\tau(0, 0) = [0, 0.1]$.

(b) Solutions to $\mathcal{H}_3$ such that $c_2 = .35$ with $\tau(0, 0) = [0, 0.1, 0.2]^\top$.

Fig. 5. Asymptotic convergence to the set $\mathcal{A}_N$ for $N \in \{2, 3\}$.

(a) Solutions to $\mathcal{H}_7$.
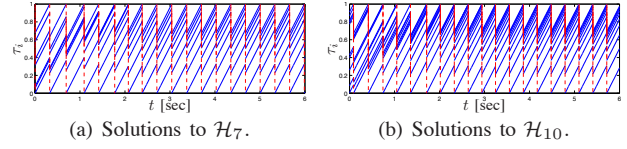
(b) Solutions to $\mathcal{H}_{10}$.

Fig. 6. Asymptotic convergence to the set $\mathcal{A}_N$ for $N \in \{7, 10\}$.

a solution to the system for 10 seconds. From the figure, it can be seen that $V_2(\tau) \approx 0.1$ at 3 seconds and 4 jumps. Then, $t + j < M$ is satisfied since $7 < 7.98$.

Figure 6 shows solutions to $\mathcal{H}_N$ that asymptotically desynchronize for $N \in \{7, 10\}$.

IV. CONCLUSION

A class of impulse-coupled oscillators was modeled using a hybrid systems framework for the study of asymptotic stability and performance. Desynchronization was recast as a set stabilization problem. An algorithm to define the desynchronization set was proposed. A Lyapunov function to certify that desynchronization is an (almost global) asymptotic stability property was proposed and, via Lyapunov theory for hybrid systems, used to establish this property for a network of N impulse-coupled oscillators.

REFERENCES

[1] C. S. Peskin. *Mathematical Aspects of Heart Physiology*. Courant Institute of Mathematical Sciences, 1975.

[2] R. E. Mirollo and S. H. Strogatz. Synchronization of pulse-coupled biological oscillators. *SIAM Journal on Applied Mathematics*, 50:1645–1662, 1990.

[3] A. Pikovsky, M. Rosenblum, and J. Kurths. *Synchronization: A Universal Concept in Nonlinear Sciences*. Cambridge University Press, 2003.

[4] A. Mauroy and R. Sepulchre. Clustering behaviors in networks of integrate-and-fire oscillators. *Chaos: An Interdisciplinary Journal of Nonlinear Science*, 18(3):037122, 2008.

[5] L. Glass and M.C. MacKey. *From Clocks to Chaos: The Rhythms of Life*. Princeton Paperbacks. Mir, 1988.

[6] R. Nagpal A. Patel, J. Desesys. Desynchronization: The theory of self-organizing algorithms for round-robin scheduling. In *Proceedings of the First Int. Conf. on Self-Adaptive and Self-Organizing Systems, '07*, pages 87–96, July 2007.

[7] J. Benda, A. Longtin, and L. Maler. A synchronization-desynchronization code for natural communication signals. *Neuron*, 52(2):347–358, October 2006.

[8] G. Pfurtscheller and F.H. Lopes da Silva. Event-related eeg/meg synchronization and desynchronization: basic principles. *Clinical Neurophysiology*, 110(11):1842–1857, 1999.

[9] M. Stopfer, S. Bhagavan, B. H. Smith, and G. Laurent. Impaired odour discrimination on desynchronization of odour-encoding neural assemblies. *Nature*, 390:70–74, November 1997.

[10] A. Nabi and J. Moehlis. Nonlinear hybrid control of phase models for coupled oscillators. In *Proceedings of the American Control Conference, 2010*, pages 922–923, July 2 2010.

[11] M. Majtanik, K. Dolan, and P.A. Tass. Desynchronization in networks of globally coupled neurons: effects of inertia. In *Proc. of 2004 IEEE Int. Joint Conference on Neural Networks*, pages 1481–86 vol.2, '04.

[12] Y.W.P. Hong, W.J. Huang, and C.C.J. Kuo. *Cooperative Communications and Networking: Tech. and System Design*. Springer, 2010.

[13] C. Liu and K. Wu. A dynamic clustering and scheduling approach to energy saving in data collection from wireless sensor networks. In *Proc. of SECON: Data Coll. Wireless Sensor Networks*, 2005.

[14] R. Goebel, R.G. Sanfelice, and A.R. Teel. *Hybrid Dynamical Systems: Modeling, Stability, and Robustness*. Princeton University Press, 2012.

[15] R. Goebel, R.G. Sanfelice, and A.R. Teel. Hybrid dynamical systems. *IEEE Control Systems Magazine*, pages 28–93, 2009.

[16] S. Phillips, R.G. Sanfelice, and R.S. Erwin. On the synchronization of two impulsive oscillators under communication constraints. In *Proc. American Control Conference, 2012*, pages 2443–2448, July 2012.